

RESEARCH ON THE GENERATION METHODS OF TOPOLOGICAL INTERLOCKING STRUCTURE ON SURFACES BASED ON GRID

SHUFAN YU¹, YUNSONG ZHANG², ZIYU TONG³ and SHULIN TIAN⁴

^{1,2,3,4}*School of Architecture and Urban Planning, Nanjing University.*

¹*522022360070@smail.nju.edu.cn, 0009-0001-0339-2703*

²*1253167018@qq.com, 0000-0001-5246-6521*

³*tzv@nju.edu.cn, 0000-0002-5872-0890*

⁴*522022360051@smail.nju.edu.cn, 0009-0008-4016-2852*

Abstract. Topological Interlocking (TI) structures have inherent advantages due to the structural characteristics of their discrete units and the diverse representation forms of these units. Previous research has summarized various methods for generating TIs on planar or curved surfaces. However, existing digital generation tools still use relatively limited methods when generating on curved surfaces. Additionally, there needs to be more control over the overall morphology, resulting in incomplete units or units that fail to meet the expected shape requirements. This paper presents a summarized method for generating TI structures based on the Truchet vault. Furthermore, it adapts the generation of TI units on curved surface grids and investigates the results of this method on various types of grids. Moreover, this paper proposes ideas for optimizing the partitioning of surface grids. Based on these ideas, specific combinations of units and grids are selected, and finite element analysis is utilized to analyze the forces and displacements of different TI unit forms. The results demonstrate that TI structures with larger unit amplitudes and higher symmetry exhibit more uniform force transmission when subjected to the same load, reducing overall stress and displacement.

Keywords. Topological Interlocking; Truchet Tiling; Finite Element Analysis (FEA); Generation Algorithm; Parametric Design; Spatial Grid.

1. Introduction

As a self-supporting masonry structure, Topological Interlocking (TI) demonstrates significant potential for applications in the construction industry, especially in digitalization, prefabrication, modularisation, and assembly trends. TI leverages its unique assembly characteristics and numerous advantages to meet the demands of these emerging trends. In TI structures, architects arrange special-shaped units in a specific manner, achieving the structure's overall stability by applying constraints to the peripheral units. This method eliminates the need

for traditional structural connection methods such as adhesives (Dyskin et al., 2003). Moreover, in the event of damage or loss of individual units within the structure, the overall stability is maintained, and only the damaged unit modules need to be replaced. Therefore, TI exhibits near-perfect recyclability as a removable, replaceable structural system (Michael et al., 2017).

In the late 17th century, Abeille invented a flat vault with stone modules arranged alternately and supporting each other. Later, Truchet built upon this concept and proposed a type of module with straight patterns to fill the gaps on the surface of Abeille's vault. Frézier further designed alternative modules resembling Truchet-style units (Lecci, F. et al., 2021) (Figure. 1). A common approach to generating TI structures is by constructing components on a densely tessellated polygonal grid, similar to Abeille-style units. Each edge of the grid unit is used to generate a plane perpendicular to the unit's face. These planes are then rotated inward and outward at the same angle, intersecting with each other to form the TI units. This method can also be extended to generate curved TI structures. (Kanel-Belov et al., 2008). Apart from that, there are generation methods based on variations of the Truchet vault and Abeille vault (M. et al., 2012). TI is also applied in architecture, primarily for constructing planar vault structures (Kevin et al., 2019). Regarding the stress analysis of TI structures, a study on the structural performance of semi-regular TI structures has revealed the relationship between geometric parameters and the forces and deformation responses of these structures (Weizmann et al., 2019).

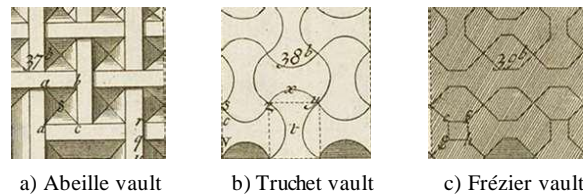


Figure 1. Drawing of top views of Abeille and Truchet vaults by Frézier, 1738

Existing digital generation tools for TI structures include the *Starfish* plugin and the *TopoRhino* plugin in Grasshopper. However, these tools still need some improvement. More research is needed regarding the generation of TI structures using other style units on curved surfaces, as the existing methods are limited to the approach proposed by Kanel-Belov et al. (2008). This limitation hinders the exploration of diverse forms and surface texture control. Additionally, these tools' generation of surface grids relies on mapping the planar grid onto a target surface. This mapping process may result in significant alterations to the shapes of certain units, leading to forms that deviate from the desired expectations and incomplete blocks along the edges. These issues can impact the overall aesthetics and structural integrity of TI structures.

Compared to Abeille-style units, Truchet-style units support each other and have interlocking relationships that restrict the sliding of unit blocks in multiple directions. Moreover, to achieve parametric generation, the method and control parameters of Truchet-style units are more intuitive than those of Frézier-style units. Consequently, this study is based on Truchet-style TI units and aims to address some of the issues in existing TI generation methods. It introduces parameter control to generate TI

structures that are more controllable and expressive. In this paper, the main control parameters studied are the amplitude and the interval of the function's period. The study also involves finite element analysis to evaluate the load-bearing performance of structures generated by combining different units and grids to provide better solutions in terms of structure (Figure. 2).

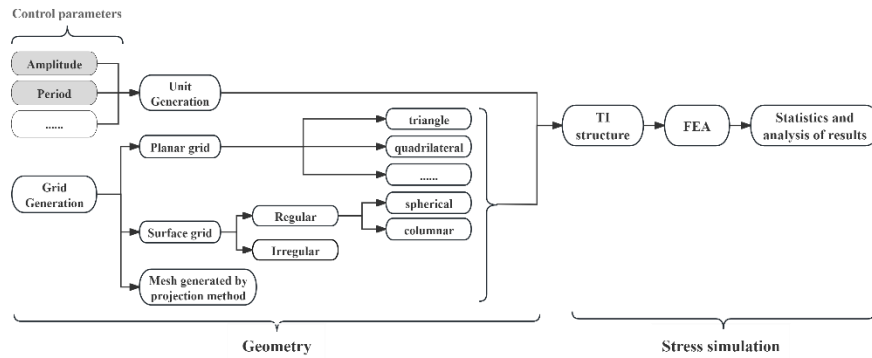


Figure 2. Flow chart

2. Parametric Generation of Units

2.1. UNIT GENERATION

After understanding the essential morphological and compositional characteristics of Truchet-style unit blocks, a digital attempt was made to generate them. The first step is to divide the edges of the unit grid. The segment points generated on each edge are then translated using the mapping relationship of the trigonometric function $y = \sin(x)$ within a certain period. The translation direction should be perpendicular to both the normal vector of the plane and the edges themselves. It is important to note that the translation direction of adjacent edges is opposite. Using an interpolation method, the translated points are connected to generate curves. Then, a distance is added by translating them along the normal vector of the grid unit surface to create the top surface. The surfaces are lofted based on the corresponding edges of the top and bottom surfaces, forming the final unit block (Figure. 3).

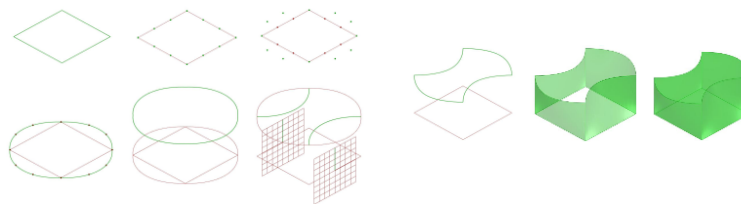


Figure 3. The process of unit generation

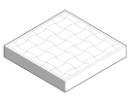
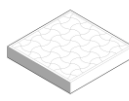
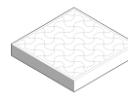
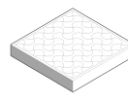
Due to symmetry, the volume of planar TI unit blocks is equal to the product of the grid unit face area and the height of the unit block. Under equal volume, this study controls the overall variation in unit morphology by manipulating the amplitude and

the interval of the function's period. These parameters influence the degree of tilt and the contact area between the unit blocks.

2.1.1. Amplitude

The control of the amplitude of the function, by varying the multiplicity of the distance traveled by the control points of each side, significantly affects the degree of curvature of the surface profile of the module. This parameter defines the curvature of each side after deformation and the degree of deformation of the unit. A smaller amplitude results in less deformation of the unit block and a smaller contact area between the blocks, while a larger amplitude leads to more significant deformation of the block and a larger contact area (Table. 1)

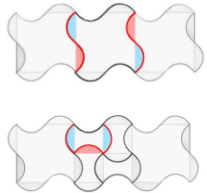
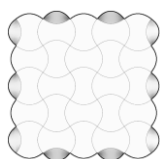
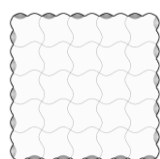
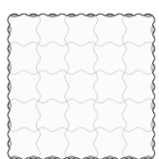
Table 1. Models with different amplitudes

A = 1	A = 2	A = 3	A = 4
			

2.1.2. Period

In the primary method, a sine function, $y = \sin(x)$, where $x \in [0, \pi]$ (half a period), is used as the variation pattern for the edges of the unit surface. By adjusting the range of values, different unit blocks can be obtained. To ensure that the modified curves can form closed loops and enclose a plane, one must keep the positions of the two endpoints of the curve fixed at the vertices of the original polygon grid. Therefore, the appropriate range of values is $x \in [0, n\pi]$, where $n \in \mathbb{N}^+$ (Table. 2). This means that when using the sine function as the variation pattern for the edges of the unit surface, the reasonable range of values for the period, denoted as X , is $X \in [0, n/2]$, where $n \in \mathbb{N}^+$.

Table 2. Models with different periods

X = 0.5	X = 1	X = 1.5	
			

It is worth noting that when $X=1$, i.e., the variation function is $y=\sin(x)$, with $x \in [0, 2\pi]$, the results generated using the primary method overlap and do not form an interlocking pattern. When X is a positive integer ($X \in \mathbb{N}^+$), the generated curves are centrally symmetric curves centered at the midpoints of the corresponding unit grid edges. The TI unit body at $X=1$ can be visualized as the assembly of four quarter-sized unit bodies corresponding to $X=0.5$. In this case, there are eight interlocking regions, where four restrict downward movement, and the other four restrict upward movement (Table. 2).

3. TI Structural Morphology

3.1. GRID GENERATION

3.1.1. Surface Grid Optimisation

Starfish will map the grid back to the original surface if the input surface has been trimmed when generating a grid for the same curved surface. As a result, the generated grid may differ significantly from the input reference surface, leading to a mismatch between the desired TI structure and the actual generated form. The controllability of the form is also affected in this case (Figure. 4).

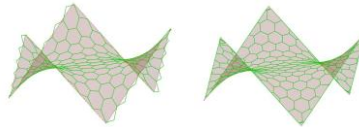


Figure 4. Surface grids with different generation methods (left: *Starfish*, right: *TopoRhino*)

TopoRhino uses a method of flattening the grid of the curved surface, aligning it with the grid, and then mapping the grid within its contour back to the curved surface. Compared to *Starfish*, the grid generated by *TopoRhino* is more aligned with the form and contour of the curved surface. However, incomplete blocks may still be at the edges of the generated grid structure (Figure. 4).

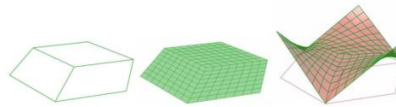


Figure 5. After the initial meshing of a complex surface, *Kangaroo* is used to find the shape of the surface grid.

A strategy can be employed for complex curved surface grids to preprocess the initial planar grid. The grid can be divided into hierarchical units based on its features, and then the *Kangaroo* plugin can be utilized to find the desired surface form. This approach enables the generation of edge units with regular arrangements and a freeform surface grid that better aligns with the principles of structural mechanics, which is crucial for subsequent TI generation (Figure. 5).

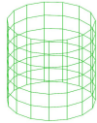
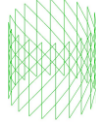
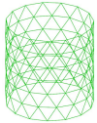
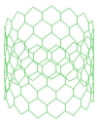
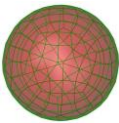





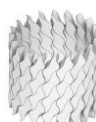
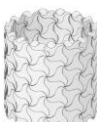


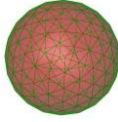
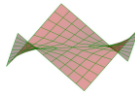
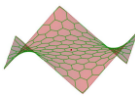
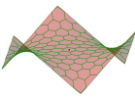
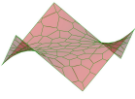
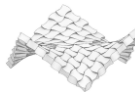
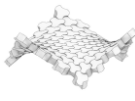

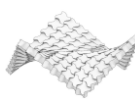
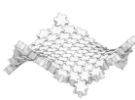
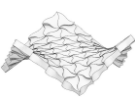
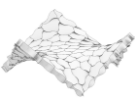
3.2. COMBINATION OF UNITS AND GRIDS

In this paper, the mentioned grids can be categorized into planar, regular, and free-form surface grids. The grid elements, respectively, consist of triangles, quadrilaterals, hexagons, and Voronoi polygons.

When the edges vary in non-centrally symmetric curve form, i.e., when the value of the period X is a non-integer, the method only applies to even-sided polygons (quadrilateral or hexagonal grids). It cannot be directly applied to triangular grids or grids composed of polygons with different numbers of sides. However, when X is an integer, the variations of individual unit block edges can be self-complementary. In this

case, the method can theoretically generate TI on grids of any form (Table. 3).

Table 3. Units applied to different types of grids

Surface grid	Columnnar	Columnnar	Columnnar	Columnnar	Spherical
Grid cell	Rectangular	Parallelogram	Triangular	Hexagonal	Quadrilateral
Grid					
$\xi=0=X$			×		
$l=X$					
Surface grid	Spherical	Hyperboloid	Hyperboloid	Hyperboloid	Hyperboloid
Grid cell	Triangular	Quadrilateral	Hexagonal	Triangular	Voronoi
Grid					
$\xi=0=X$	×			×	×
$l=X$					

4. Force Simulation

Using finite element analysis (FEA), we simulate the load-bearing performance of TI structures with different amplitudes and periods to investigate the relationship between their geometric form and the forces and structural deformations. The individual structure consists of 49 unit blocks and their constrained boundary. The unit blocks are generated using a 7*7 orthogonal quadrilateral grid, where each grid cell has dimensions of 10cm*10cm. The height of each unit block is 10cm. The overall size of

the structure is 90cm*90cm*10cm, with constraints applied to its four sides. To ensure consistent load conditions during simulation, a pressure of 500N is applied within a square area of 10cm*10cm at the center of the structure.

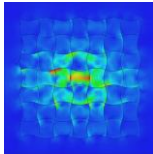
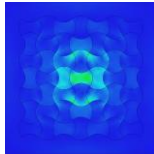
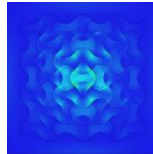
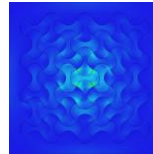
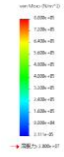
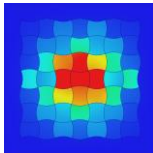
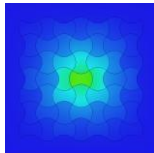
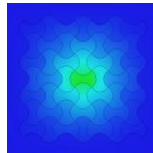
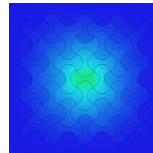
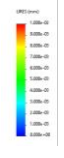
Secondly, select the same freeform surface and compare the optimized grid's TI structure with the grid's TI structure determined by the mapping method to evaluate which approach yields a more reasonable structure.

The material for simulation is set as concrete, with the following properties: mass density of 2300 kg/m³, Young's modulus of 3e+4 GPa, Poisson's ratio of 0.18, shear strength of 1.27e+4 GPa, and yield strength of 20 GPa. The unit relationship is set as contact, with a friction coefficient of 0.05.

The evaluation criteria for the results can be based on the numerical changes in the maximum displacement, average displacement, maximum stress, and average stress.

4.1. AMPLITUDE

Table 4. Comparison of simulation results for models with different amplitudes

Amplitude	A=1	A=2	A=3	A=4	Legend
Von-mises stresses					
Max (Pa)	5.38E+04	2.60E+04	2.42E+04	2.48E+04	
Displacement					
Max (mm)	3.23E-02	5.96E-03	4.87E-03	3.95E-03	

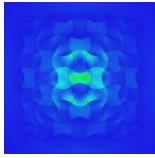
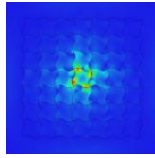
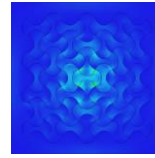
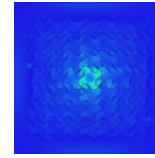
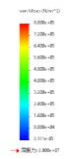
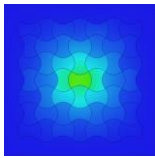
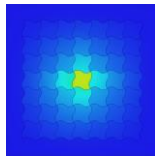
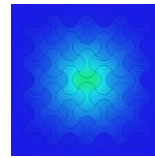
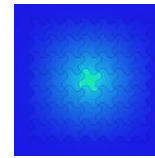
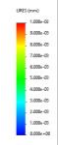
The four groups of models are selected with varying amplitudes A, with an interval of 1. The results indicate that as the amplitude increases, the maximum displacement and overall displacement decrease, and the maximum Von Mises stresses gradually decrease as well (Table. 4). The force tends to transmit in the direction of the convex curve of the unit block, resulting in compression on the surrounding unit blocks. When the amplitude A is increased to 4, the average displacement of the overall structure decreases by 65.3% compared to A=1. Similarly, the average stress decreases by 53.9% in this case.

4.2. PERIOD

In the case of the same amplitude, we compare the load-bearing performance of TI structures with periods $X=0.5$ and $X=1$. For $A=2$, $X=1$ compared to $A=2$, $X=0.5$, the contact area between unit blocks decreases, but the average displacement decreases by 17.7%, the maximum displacement increases by 18%, and the average stress decreases by 4.1%. The maximum stress in the central block increases by 194.4%. For $A=4$, $X=1$ compared to $A=4$, $X=0.5$, the average displacement decreases by 17.0%, the maximum displacement decreases by 11.6%, and the average stress decreases by 27.2%. The maximum stress in the central block decreases by 25.6% (Table. 5).

TI structures generated by this method tend to apply forces to the surrounding units along the convex parts of the curved edges. Therefore, in the case of $X=1$, the forces are transmitted through all the side faces to the surrounding units, resulting in a more stable overall force transmission compared to $X=0.5$. However, it is essential to note that the stress in the centrally loaded unit block may increase at the corners. When designing TI structures, it is crucial to consider multiple factors and select appropriate structural parameters to ensure a balanced design.

Table 5. Comparison of simulation results for models with different periods

Amplitude	A=2, X=0.5	A=2, X=1	A=4, X=0.5	A=4, X=1	Legend
Von-mises stresses					
Max (Pa)	2.33E+05	6.86E+05	2.89E+05	2.15E+05	
Displacement					
Max (mm)	5.96E-03	7.03E-03	3.95E-03	3.49E-03	

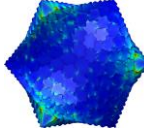

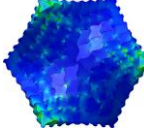
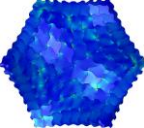

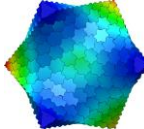
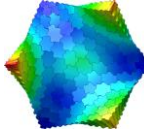
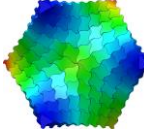
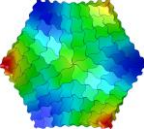
4.3. SURFACE GRID

In this section, a comparison is made between the optimized surface grid and the hexagonal projection grid. Since it is difficult to apply the same load to both models, the focus is on testing the self-bearing effect of the models. The models will be uniformly scaled, and a portion of the base will be truncated to ensure a more stable placement, reducing the impact on the simulation results. The corners of the base will be fixed while keeping the other parameters consistent with the previous discussion.

The experimental results show that, for the same surface, the locations with the

largest displacements are observed at the corners of the top surface and the central portion of the surface. The maximum displacement difference between the two models is less than 0.1%. The displacement results are consistent with the geometric characteristics of each grid. Six TI unit blocks are joined together in the center of the optimized grid. Compared to a single unit block at the center of the hexagonal projection grid, this model is more prone to downward displacement at the center point of the curved surface. As a result, the average displacement of the optimized grid is increased by 24.1% compared to the hexagonal grid. However, the maximum stress in the optimized grid TI structure decreases by 49.4%, indicating that the more uniform and complete unit blocks in the optimized grid allow for a more even distribution of forces within the structure (Table. 6).

Table 6. Comparison of simulation results for models generated from different surface grids

Amplitude	Grid generated by projection		Optimized grid		Legend
Von-mises stresses					
Displacement					

5. Conclusion

This article summarises the generation method for Truchet-style TI structures. Two groups of factors determine the final results: 1) Input grid: The morphology of the base grid determines the overall shape of the generated TI structure. On the other hand, the structure of the grid determines the organization and order of the TI unit blocks. Different grid morphologies and structures can result in different types and arrangements of TI unit blocks; 2) Generation parameters for the unit: Different parameters have different applicability to grid types, the morphology of the generated units, and the arrangement effects. Within this framework, selecting different parameter controls based on specific objective requirements for generating TI structures is possible.

FEA was conducted based on this, studying the displacement and stress distribution characteristics of TI structures under different parameters. Firstly, the amplitude has a significant impact on the overall structural load. A more considerable amplitude results in smaller displacement and stress. However, it should be noted that the distortion of the edges and corners of the unit blocks may increase, which may not be conducive to subsequent production. On the other hand, a smaller amplitude has a more significant influence from frictional forces, while a larger amplitude tends to exert pressure and support on the surrounding unit blocks.

In addition, the period of the units also plays a role. When $X \geq 1$, the TI structure exhibits better symmetry, resulting in a more uniform distribution of forces. However,

certain unit blocks may stress their edges and corners more.

Each has its advantages for different grid divisions on the same curved surface. The projection grid exhibits smaller overall displacement changes, but it may have more incomplete or missing unit blocks at the edges, which can be disadvantageous for structural load-bearing. The divided and optimized grid has more complete unit blocks and a more uniform distribution of forces but may exhibit larger overall displacement changes.

One can choose a suitable combination of unit morphology and curved surface grid division by considering load-bearing capacity, structural integrity, displacement limitations, stress distribution, symmetry, and production feasibility. This selection is crucial in the subsequent construction and production processes.

References

- Akleman, E., Krishnamurthy, V. R., Fu, C. A., Subramanian, S. G., Ebert, M., Eng, M., ... & Panchal, H. (2020). Generalized Abeille tiles: Topologically interlocked space-filling shapes generated based on fabric symmetries. *Computers & Graphics*, 89, 156–166. <https://doi.org/10.1016/j.cag.2020.05.016>
- Dyskin, A. V., Estrin, Y., Kanel-Belov, A. J., & Pasternak, E. (2003). Topological interlocking of platonic solids: A way to new materials and structures. *Philosophical magazine letters*, 83(3), 197-203. <https://doi.org/10.1080/0950083031000065226>
- Gata, K. M., Mueller, C., & Valiente, E. E. (2019, October). Designing strategies for topological interlocking assemblies in architecture. *Flat vaults*. In *Proceedings of IASS Annual Symposia (Vol. 2019, No. 15, pp. 1–8)*. International Association for Shell and Spatial Structures (IASS).
- Kanel-Belov, A. J., Dyskin, A. V., Estrin, Y., Pasternak, E., & Ivanov-Pogodaev, I. A. (2008). Interlocking of convex polyhedra: towards a geometric theory of fragmented solids. *arXiv preprint arXiv:0812.5089*. <https://doi.org/10.48550/arXiv.0812.5089>
- Kurucu, A. T., & İlerisoy, Z. Y. (2023). Structural Performance of Topologically Interlocked Flat Vaults According to Joint Details. *Periodica Polytechnica Architecture*, 54(1), 1-11. <https://doi.org/10.3311/PPar.19509>
- Lecci, F., Mazzoli, C., Bartolomei, C., & Gulli, R. (2021). Design of flat vaults with topological interlocking solids. *Nexus Network Journal*, 23(3), 607-627. <https://doi.org/10.1007/s00004-020-00541-w>
- Pfeiffer, A., Lesellier, F., & Tournier, M. (2020). Topological interlocking assemblies experiment. In *Impact: Design With All Senses: Proceedings of the Design Modelling Symposium, Berlin 2019 (pp. 336-349)*. Springer International Publishing. https://doi.org/10.1007/978-3-030-29829-6_27
- Weizmann, M., Amir, O., & Grobman, Y. J. (2017). Topological interlocking in architecture: A new design method and computational tool for designing building floors. *International journal of architectural computing*, 15(2), 107-118. <https://doi.org/10.1177/1478077117714913>
- Weizmann, M., Amir, O., & Grobman, Y. J. (2019, April). Structural performance of semi-regular topological interlocking assemblies. In *Proceedings of the Symposium on Simulation for Architecture and Urban Design (pp. 1-7)*.